

## Pulse propagation in spatially dispersive media

Ashok Puri\* and Joseph L. Birman

*Physics Department, City College, City University of New York, New York, New York 10031*

(Received 1 June 1982)

The propagation of a Gaussian electromagnetic (optical) pulse with center frequency  $\bar{\omega}$  (laser) through a spatially dispersive exciton-polariton medium is investigated by a combination of analytical and numerical methods. The analysis used extends previous work by Garrett and McCumber to the multiwave coupled exciton-polariton case. With the assumption of normal incidence on a semi-infinite medium, laser frequencies very close to exciton resonance and far from resonance are studied. Numerical results are obtained for power spectrum  $P(z, \omega)$  and amplitude profile  $f(z, t)$  for parameters suitable to CdS 1S *A* exciton (a fairly typical semiconductor). For pulses with  $\Gamma\tau \gg 1$  or  $\Gamma\tau \sim 1$  the pulse remains essentially Gaussian, and its peak propagates with velocity close to the classical group velocity  $v_{gj} = (d\omega_j/dk_r)$ , where  $j$  is the polariton branch index and  $k_r$  is the real part of the propagation wave number. The power spectrum shows a crossover from lower to upper branch as the laser frequency is varied through resonance. Some comparison with experiments on CuCl, GaAs, CdSe, and CdS semiconductors is also given.

## I. INTRODUCTION

When an electromagnetic wave propagates through a medium of refractive index  $n$ , the phase velocity is given by  $c/n$  and the group velocity is given by<sup>1,2</sup>

$$v_g = \frac{c}{n + \omega \frac{dn}{d\omega}} \quad (1)$$

In the region of normal dispersion  $dn/d\omega > 0$ , and the group velocity,  $v_g$  is less than the phase velocity  $v_p$ . On the other hand,  $dn/d\omega < 0$  in the region of anomalous dispersion and  $v_g$  could exceed the velocity of light. The common belief is that concept of group velocity breaks down in this case.

Sommerfeld and Brillouin<sup>2</sup> in their classical work show that in an absorbing medium, for an incident pulse of form

$$f(t) = \theta(t) \sin \omega t,$$

the original pulse is distorted. The first precursors of the pulse travel at the vacuum speed of light  $c$ , but the main pulse arrives at the signal velocity  $v_s < c$ . Loudon<sup>3</sup> showed that the electromagnetic energy travels at the energy velocity  $v_E < c$ . Here the energy velocity  $v_E$  is defined as the magnitude of the ratio of Poynting flux and electromagnetic-energy density. Garrett and McCumber<sup>4</sup> in an important paper studied the propagation of steady-state Gaussian pulses through an absorbing medium, in the region of strong absorption. They predicted that

under assumptions which can be readily satisfied, the peak of the pulse propagates with the group velocity  $v_g$ , even when  $v_g > c$  or  $\pm\infty$ . Related theoretical work was reported by Crisp<sup>5</sup> who used a different representation of the amplitude of the electromagnetic field, and also obtained the result that the peak of the pulse in absorbing media can travel with the group velocity. Chu and Wong<sup>6</sup> performed a time-of-flight experiment on GaP:N and have recently verified Garrett and McCumber's predictions on the propagation velocity of the peak.

Recently there has been considerable interest in studies of optical properties of bounded crystals which, near an exciton resonance, exhibit spatial dispersion (i.e., GaAs, CuCl, CdSe, CdS,<sup>7-10</sup> and others). As is well known in these types of crystals, exciton polaritons are formed when light enters the crystal. One characteristic effect of spatial dispersion is that at any frequency several waves travel, each with different phase velocity. These are coupled exciton-photon waves. The physical polariton is the correct linear combination of these waves, with coefficients of the linear combinations to be determined by relevant additional boundary conditions.<sup>11-13</sup> Recently we studied the propagation of electromagnetic energy in such media.<sup>14</sup>

In Sec. II we employ the Garrett and McCumber-type of analysis to study Gaussian pulse propagation in spatially dispersive media, far from exciton resonance  $\omega_0$  as well as in the regime  $\omega_0 < \bar{\omega} < \omega_l$ . In Sec. III we give numerical results for pulse propagation through spatially dispersive

media close to an exciton resonance for CdS parameters. Finally, Sec. IV is devoted to a brief discussion of pulse propagation near to and away from exciton resonance.

## II. PULSE PROPAGATION THROUGH NONLOCAL SPATIALLY DISPERSIVE MEDIA

Let us consider a Gaussian pulse incident on the semi-infinite  $z \geq 0$  spatially dispersive medium. The amplitude of the field at the point  $z$  and time  $t$  is given by

$$f(z,t) = \tau(2\pi)^{-1/2} \int_{-\infty}^{\infty} d\omega e^{-i\omega t} \sum_{j=1}^2 f_j(z,\omega), \quad (2a)$$

where

$$f_j(z,\omega) = A_j(\omega) e^{ik_j(\omega)z} e^{-(\omega - \bar{\omega})^2 \tau^2 / 2}. \quad (2b)$$

Here  $\bar{\omega}$  is the central frequency of the Gaussian and  $\tau^{-1}$  is the half width of the pulse;  $j=1,2$  correspond to upper and lower polaritons (UP and LP), respectively;  $k_j$  is the solution of the dispersion equation for transverse electromagnetic waves  $k^2 = k_0^2 \epsilon(\omega, k)$ ;  $\epsilon(\omega, k)$  is the dielectric function for spatially dispersive medium and is given in the "dielectric approximation" by<sup>11-13</sup>

$$\epsilon(\omega, k) = \epsilon_0 + \frac{4\pi\alpha_0\omega_0^2}{\omega_0^2 - \omega^2 - i\omega\Gamma + bk^2}. \quad (3)$$

Here  $\epsilon_0$ ,  $4\pi\alpha_0$ ,  $\omega_0$ , and  $\Gamma$  are background dielectric constant, oscillator strength, exciton-resonance frequency and damping constant, respectively,  $b$  is given by  $\hbar\omega_0/m^*$ , with  $m^*$  being the exciton mass.

In Eq. (2)  $A_j(\omega)$  are coupling constants to be determined by the full set of boundary conditions (Maxwell's plus additional boundary conditions<sup>11-13</sup>).

For frequency regimes  $\bar{\omega}/\omega_0 \gg 1$ ,  $\bar{\omega}/\omega_0 \ll 1$ , and  $\omega_0 < \bar{\omega} < \omega_l$  there is effectively a single polariton propagating and the Garrett and McCumber analysis can be applied. We discuss these regimes in this section. Assuming  $\Gamma\tau \gg 1$ , we can carry out expansion of the wave vector  $k(\omega)$  around  $\bar{\omega}$ ,

$$k(\omega) = k(\bar{\omega}) + (\omega - \bar{\omega}) \left. \frac{dk}{d\omega} \right|_{\bar{\omega}} + \frac{1}{2} (\omega - \bar{\omega})^2 \left. \frac{d^2k}{d\omega^2} \right|_{\bar{\omega}} + \dots \quad (4)$$

For the oscillator model this series converges<sup>4</sup> for  $(\omega - \bar{\omega})^2 \tau^2 \leq 1$  and  $\Gamma\tau \gg 1$ . Thus we expand up to second order in Eq. (4). Putting Eq. (4) in Eq. (2) we get

$$f(z,t) = \frac{\tau}{\sqrt{2\pi}} \int_{-\infty}^{\infty} d\omega e^{-i\omega t} \sum_{j=1}^2 A_j(\omega) \exp \left[ i \left[ k_j(\bar{\omega}) + (\omega - \bar{\omega}) \left. \frac{dk_j}{d\omega} \right|_{\bar{\omega}} + \frac{(\omega - \bar{\omega})^2}{2} \left. \frac{d^2k_j}{d\omega^2} \right|_{\bar{\omega}} \right] z \right] \times \exp \{ -[(\omega - \bar{\omega})^2 \tau^2 / 2] \}.$$

Substituting  $(\omega - \bar{\omega}) = u$  we get

$$f(z,t) \simeq \frac{\tau}{\sqrt{2\pi}} \sum_{j=1}^2 A_j(\bar{\omega}) \exp[i(k_j(\bar{\omega})z - \bar{\omega}t)] \times \int_{-\infty}^{\infty} du \exp \left[ -iut - u^2 \frac{\tau^2}{2} + i \left[ u \left. \frac{dk_j}{d\omega} \right|_{\bar{\omega}} + u^2 \left. \frac{d^2k_j}{d\omega^2} \right|_{\bar{\omega}} \right] z \right]. \quad (5)$$

Carrying out the integration we get

$$f(z,t) = \sum_{j=1}^2 \left[ 1 - \frac{zi}{\tau^2} \left. \frac{d^2k_j}{d\omega^2} \right|_{\bar{\omega}} \right]^{-1/2} A_j(\bar{\omega}) \exp[i(k_j(\bar{\omega})z - \bar{\omega}t)] \times \exp \left[ - \left[ t - z \left. \frac{dk_j}{d\omega} \right|_{\bar{\omega}} \right]^2 / 2\tau^2 \left[ 1 - \frac{zi}{\tau^2} \left. \frac{d^2k_j}{d\omega^2} \right|_{\bar{\omega}} \right] \right] = \sum_{j=1}^2 f_j(z,t). \quad (6)$$

Next we proceed to discuss various limiting cases. We employ an expansion of  $k_j(\omega)$  for various cases, following Frankel and Birman.<sup>15</sup>

*Case 1:  $\bar{\omega}/\omega_0 \gg 1$ .* Above the exciton resonance, i.e., in the limit  $\bar{\omega}/\omega_0 \gg 1$ , the dispersion  $k_j(\omega)$  is given by

$$k_1(\omega) = \sqrt{\epsilon_0} \frac{\omega}{c} - \frac{c}{b\sqrt{\epsilon_0}} \frac{\beta^2 \omega_0^2}{(2\beta\omega + i\Gamma)}, \quad (7a)$$

$$k_2(\omega) = \frac{\omega}{\sqrt{b}} + \frac{i\Gamma}{2\sqrt{b}} - \frac{\omega_0^2}{\sqrt{b}(2\omega - i\Gamma)}, \quad (7b)$$

where  $\beta = 4\pi\alpha_0 b/c^2$ . Putting (7a) in Eq. (6) we get

$$f_1(z, t) = \frac{1}{\sqrt{M}} \exp[-(\Delta_1 + i\Delta_2)A_1(\bar{\omega})], \quad (8)$$

where

$$M = \left[ \left( 1 + \frac{z}{\tau^2} \frac{8c\beta^4 \omega_0^2}{b} \Gamma \frac{(12\beta^2 \bar{\omega}^2 - \Gamma^2)}{[(2\beta\bar{\omega})^2 + \Gamma^2]^3} \right) + i \left( \frac{z}{\tau^2} \frac{8c\beta^4}{b} \omega_0^2 \frac{(2\beta\bar{\omega})^2 - 6\beta\bar{\omega}\Gamma^2}{[(2\beta\bar{\omega})^2 + \Gamma^2]^3} \right) \right], \quad (9a)$$

$$\Delta_1 = \frac{(t - \alpha)^2}{2\tau_2^2} + \left[ \frac{U}{\gamma} + V \right] \frac{1}{2\tau_1^2} + W, \quad (9b)$$

$$\tau_2^2 = \gamma^{-1} \tau_1^2, \quad (9c)$$

$$\tau_1^2 = \tau^2 |M|^2, \quad (9d)$$

$$\gamma = \left[ 1 + \frac{z}{\tau^2} \frac{8c\beta^4 \omega_0^2}{b} \Gamma \frac{12\beta^2 \bar{\omega}^2 - \Gamma^2}{[(2\beta\bar{\omega})^2 + \Gamma^2]^3} \right], \quad (9e)$$

and  $\alpha, U, V, W$ , and  $\Delta_2$  are functions of  $\bar{\omega}, z$ , and parameters appearing in the dielectric function  $\epsilon(\omega, \mathbf{k})$  in Eq. (3).

Similarly putting (7b) in Eq. (6) we get

$$f_2(z, t) = \frac{1}{\sqrt{M'}} \exp[-(\Delta'_1 + i\Delta'_2)A_2(\bar{\omega})], \quad (10)$$

where

$$M' = \left[ \left( 1 - \frac{z}{\tau^2} \frac{8\omega_0^2}{\sqrt{b}} \Gamma \frac{(12\bar{\omega}^2 - \Gamma^2)}{[(2\bar{\omega})^2 + \Gamma^2]^3} \right) + i \left( \frac{z}{\tau^2} \frac{8\omega_0^2}{\sqrt{b}} \frac{(2\bar{\omega})^3 - 6\bar{\omega}\Gamma^2}{[(2\bar{\omega})^2 + \Gamma^2]^3} \right) \right],$$

$$M' = \left[ \left( 1 - \frac{z}{\tau^2 2\sqrt{2b}} \frac{\xi(\gamma^3 - 3\gamma\delta^2) + \eta(\delta^3 - 3\gamma^2\delta)}{(\gamma^2 + \delta^2)^3} \right) + i \left( \frac{z}{\tau^2 2\sqrt{2b}} \frac{\eta(\gamma^3 - 3\gamma\delta^2) - \xi(\delta^3 - 3\gamma^2\delta)}{(\gamma^2 + \delta^2)^3} \right) \right], \quad (15a)$$

$$\Delta'_1 = \frac{(t - \alpha')^2}{2\tau_2'^2} + \left[ \frac{U'}{\gamma'} + V' \right] \frac{1}{2\tau_1'^2} + W', \quad (15b)$$

$$\tau_2'^2 = \tau_1'^2 \gamma'^{-1}, \quad (15c)$$

$$\tau_1'^2 = \tau^2 |M'|^2, \quad (15d)$$

$$\Delta'_1 = \frac{(t - \alpha')^2}{2\tau_2'^2} + \left[ \frac{U'}{\gamma'} + V' \right] \frac{1}{2\tau_1'^2} + W', \quad (11a)$$

$$\Delta'_1 = \frac{(t - \alpha')^2}{2\tau_2'^2} + \left[ \frac{U'}{\gamma'} + V' \right] \frac{1}{2\tau_1'^2} + W', \quad (11b)$$

$$\tau_2'^2 = \gamma'^{-1} \tau_1'^2, \quad (11c)$$

$$\tau_1'^2 = \tau^2 |M'|^2, \quad (11d)$$

$$\gamma' = \left[ 1 - \frac{z}{\tau^2} \frac{8\omega_0^2}{\sqrt{b}} \Gamma \frac{12\bar{\omega}^2 - \Gamma^2}{[(2\bar{\omega})^2 + \Gamma^2]^3} \right], \quad (11e)$$

and  $\alpha', U', V', W'$ , and  $\Delta'_2$  are functions of  $\bar{\omega}, z$ , and parameters appearing in dielectric function  $\epsilon(\omega, k)$ .

Case 2:  $\omega_0 < \bar{\omega} < \omega_l$ . In the gap region  $\omega_0 < \bar{\omega} < \omega_l$  there is one polariton mode propagating in the medium and the amplitude of this mode can be calculated by considering the approximate form of dispersion in the gap

$$k_2(\omega) = \frac{1}{\sqrt{b}} [(\omega - \bar{\omega})(\omega + \bar{\omega})]^{1/2}, \quad (12)$$

where

$$\bar{\omega} = -\frac{i\Gamma}{2} + \omega_0(1 + \Delta - \Gamma^2/2\omega_0^2)^{1/2}$$

and

$$\Delta = b\epsilon_0/c^2.$$

In the limit  $\omega \approx \bar{\omega}$ ,

$$k_2(\omega) = \left[ \frac{2\bar{\omega}}{b} \right]^{1/2} (\omega - \bar{\omega})^{1/2}. \quad (13)$$

Using Eqs. (13) and (6) we can write the amplitude in the gap region as

$$f_2(z, t) = \frac{1}{\sqrt{M'}} \exp[-(\Delta'_1 + i\Delta'_2)A_2(\bar{\omega})], \quad (14)$$

where

$$\gamma' = \left[ 1 - \frac{z}{\tau^2 2\sqrt{2b}} \frac{\xi(\gamma^3 - 3\gamma\delta^2) + \eta(\delta^3 - 3\gamma^2\delta)}{(\gamma^2 + \delta^2)^3} \right], \quad (15e)$$

and  $\gamma, \delta, \eta, \xi, U', V', W'$ , and  $\Delta'_2$  are functions of  $\bar{\omega}, z$ , and parameters appearing in dielectric function.

Case 3:  $\bar{\omega}/\omega_0 \ll 1$ . Finally, away from resonance (below resonance), i.e.,  $\bar{\omega}/\omega_0 \ll 1$ , there is only one propagating polariton branch in this limit; the dispersion relation is approximated as

$$k_2(\omega) = q \frac{\omega}{\sqrt{b}} + \frac{i\omega^2 \Gamma}{4q\omega_0^2 \sqrt{b}} + \frac{\omega^3}{8q\omega_0^2 \sqrt{b}}, \quad (16)$$

where

$$q = \left[ \frac{b\epsilon_0}{c^2} \left[ 1 + \frac{4\pi\alpha_0}{\epsilon_0} \right] - \Gamma^2/4\omega_0^2 \right]^{1/2}.$$

Again as in previous cases putting Eq. (16) in (6) we obtain the amplitude of the polariton as

$$f_2(z, t) = \frac{1}{\sqrt{M}} \exp[-(\Delta'_1 + i\Delta'_2)A_2(\bar{\omega})], \quad (17)$$

where

$$M' = \left[ \left[ 1 + \frac{\Gamma z}{\tau^2} \frac{1}{2q\omega_0^2 \sqrt{b}} \right] - i \left[ \frac{3}{4} \frac{z}{\tau^2} \frac{\bar{\omega}}{q\omega_0^2 \sqrt{b}} \right] \right], \quad (18a)$$

$$\Delta'_1 = \frac{(t - \alpha')^2}{2\tau_2'^2} + \left[ \frac{U'}{\gamma'} + V' \right] \frac{1}{2\tau'^2} + W', \quad (18b)$$

$$\tau_2'^2 = \gamma'^{-1} \tau_1'^2, \quad (18c)$$

$$\tau_1'^2 = \tau^2 |M'|^2, \quad (18d)$$

$$\gamma' = \left[ 1 + \frac{z\Gamma}{2\tau^2 q \omega^2 \sqrt{b}} \right], \quad (18e)$$

and  $\alpha', U', Y', V', W'$  are functions of  $\bar{\omega}, z$ , and parameters appearing in the function  $\epsilon(\omega, k)$ .

### III. PULSE PROPAGATION CLOSE TO $\omega_1(\bar{\omega} \gtrsim \omega_1)$

In the case of nonlocal spatially dispersive media, at each frequency there is more than one propagating mode. In the frequency region just above  $\omega_1$  there are two polariton modes which couple strongly to each other. Now we concentrate on this frequency region. We have been unable to obtain analytical results and thus we perform a numerical study. We compute the power spectrum  $P(z, \omega)$  where

$$\begin{aligned} P(z, \omega) &= 2\pi\tau^2 |f(z, \omega)|^2 \simeq 2\pi\tau^2 (|f_1(z, \omega)|^2 + |f_2(z, \omega)|^2) \\ &= 2\pi\tau^2 \{ |A_1(\omega)|^2 \exp[-(\omega - \bar{\omega})\tau^2 - 2 \text{Im}k_1(\omega)z] \\ &\quad + |A_2(\omega)|^2 \exp[-(\omega - \bar{\omega})\tau^2 - 2 \text{Im}k_2(\omega)z] \}. \end{aligned} \quad (19)$$

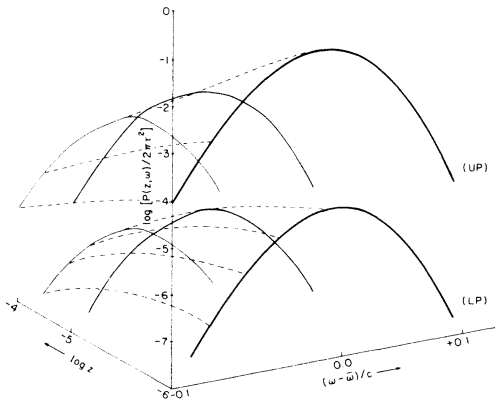


FIG. 1.  $\log_{10}[P(z, \omega)/2\pi\tau^2]$  for  $\Gamma\tau \gg 1$  case is plotted against  $(\omega - \bar{\omega})/c$  for various crystal thicknesses  $z$ , ranging from  $10^{-6}$  to  $10^{-4}$  cm. In the figure,  $\log_{10}z$  is taken. Parameters used for CdS are defined in the text.

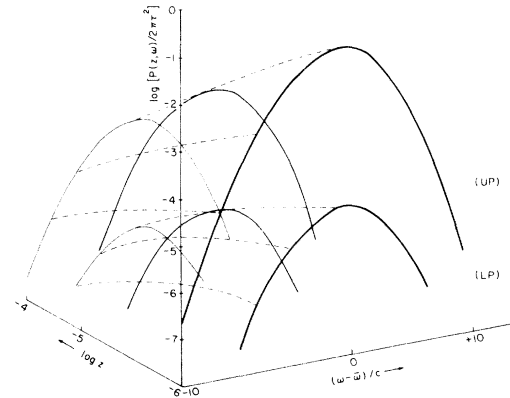


FIG. 2. Same as Fig. 1 for the  $\Gamma\tau = 1$  case.

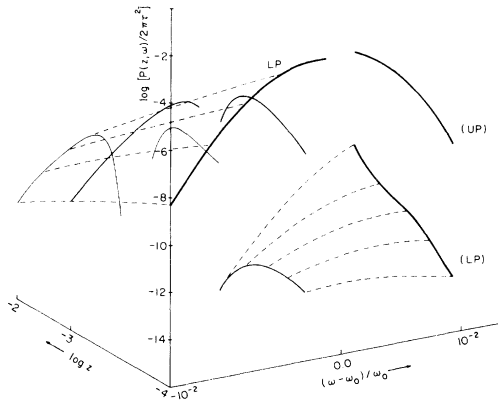


FIG. 3.  $\log_{10}[P(z,\omega)/2\pi\tau^2]$  for  $\Gamma\tau \ll 1$  case is plotted against  $(\omega - \omega_0)/\omega_0$  for various crystal thicknesses  $z$ , ranging from  $10^{-4}$  to  $10^{-2}$  cm. In the figure,  $\log_{10}z$  is taken. Parameters used for CdS are defined in text.

As an illustrative case, we consider CdS, and we used parameters  $\Gamma/2\omega_0 = 10^{-5}$ ,  $h\omega_0 = 2.55$  eV,  $m^* = 0.9m_e$ ,  $\epsilon_0 = 8$ , and  $4\pi\alpha_0 = 0.0125$ , respectively. We consider three cases, namely,  $\Gamma\tau \gg 1$ ,  $\Gamma\tau = 1$ , and  $\Gamma\tau \ll 1$ . For each case  $\tau$  is taken as 0.1 psec, 13 psec, and  $10^{-9}$  sec, respectively. Figures 1–3 show computed power spectra corresponding to these cases. Figure 4 shows the power spectrum corresponding to  $\Gamma\tau \ll 1$  very close to exciton resonance.

Next, using Eq. (2) the amplitude  $f(z,t)$  is computed for various cases, namely,  $\Gamma\tau \gg 1$ ,  $\Gamma\tau = 1$ , and  $\Gamma\tau \ll 1$ , respectively.  $\log_{10}|f_1(z,t)|$  and  $\log_{10}|f_2(z,t)|$  are plotted in each case against time  $t$  for various crystal thicknesses  $z$  in Figs. 5–7, respectively. For all the numerical studies (Figs. 1–7)  $\bar{\omega}$  is taken slightly above  $\omega_1$ , i.e.,

$$\bar{\omega} = \omega_0(1 + 10^{-3}) \gtrsim \omega_1$$

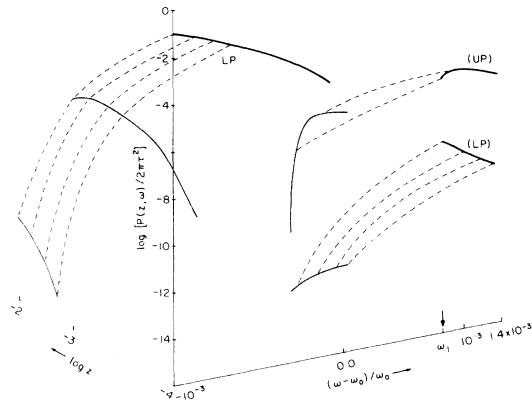


FIG. 4. Same as Fig. 3 but very close to resonance, showing crossover from LP to UP at  $\omega_1$ .

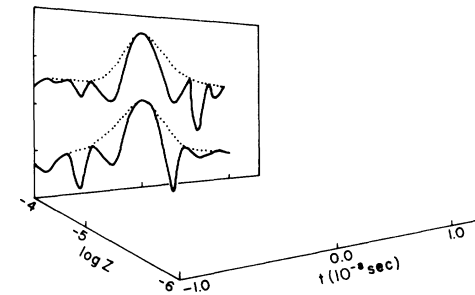
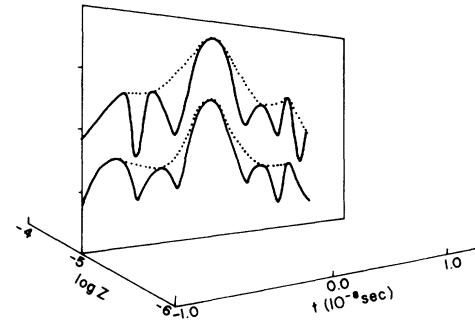
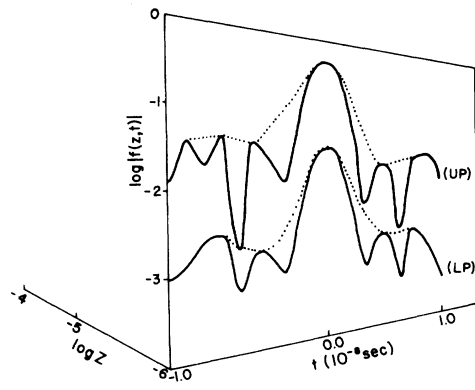


FIG. 5.  $\log_{10}|f(z,t)|$  for  $\Gamma\tau \gg 1$ , case is plotted against time  $t$  for various crystal thicknesses  $z$ , ranging from  $10^{-6}$  to  $10^{-4}$  cm. These are shown on separate plots. Parameters for CdS are defined in the text.

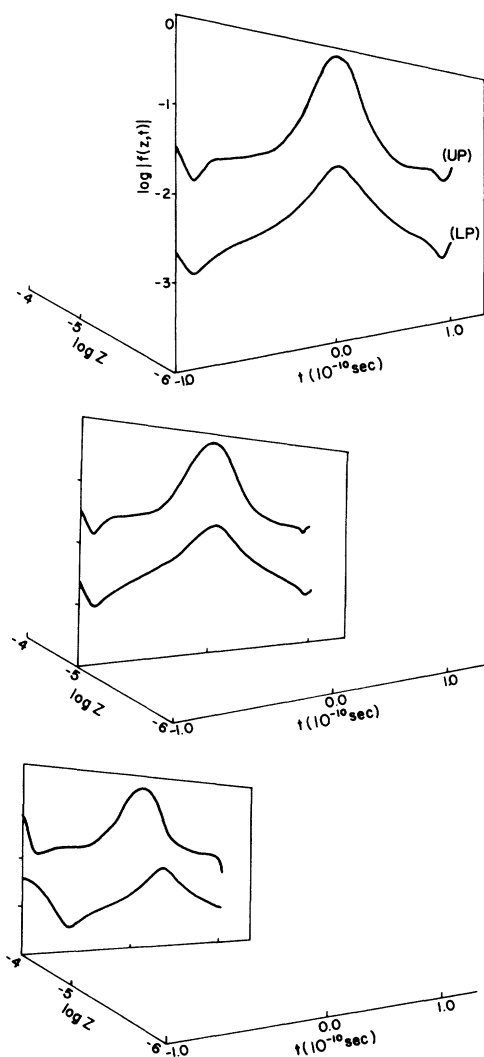
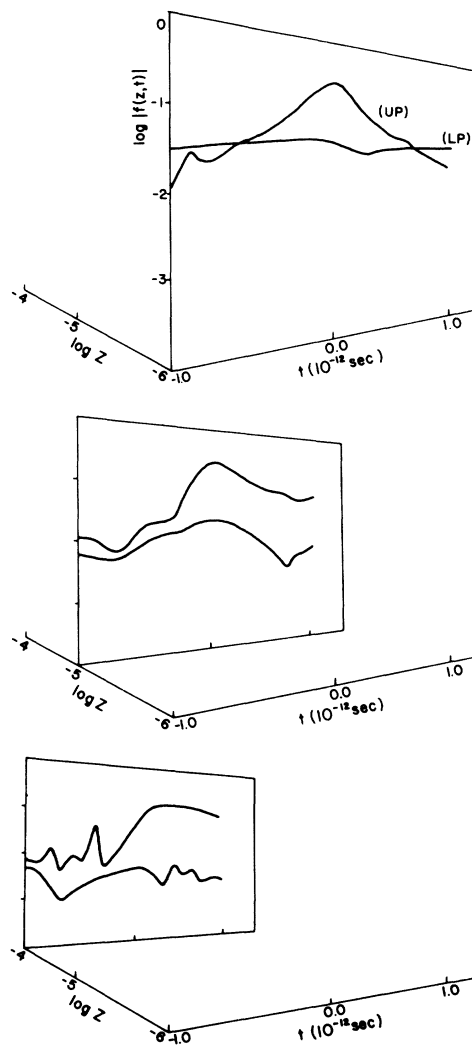
so that the effect of both polariton UP and LP can be incorporated.

We also studied the pulse shape for the various cases mentioned above. The fixed value of crystal thickness, namely,  $z = 1 \mu\text{m}$ ,  $f(z,t)$ , is computed for upper and lower polaritons as a function of time as we vary the laser frequency  $\bar{\omega}$  across the resonance. Figures 8–10 demonstrate plots for various cases as we sweep laser frequency  $\bar{\omega}$  from

$$\omega_0(1 - 10^{-2}) < \omega_1$$

to

$$\omega_0(1 + 10^{-2}) > \omega_1.$$

FIG. 6. Same as Fig. 5 for  $\Gamma\tau=1$ .FIG. 7. Same as Fig. 5 for  $\Gamma\tau \ll 1$ .

Figures 11–13 show the corresponding plots for  $\bar{\omega}$  very close to resonance, ranging from

$$\omega_0(1-10^{-3}) \lesssim \omega_l$$

to

$$\omega_0(1+10^{-3}) \gtrsim \omega_l.$$

A finer scale is used in those figures. The quantity  $S$  appearing in the Figs. 8–13 is the reduced frequency  $(\omega - \omega_0)/\omega_0$ .

#### IV. DISCUSSION

In Sec. II we presented results of an analysis of Gaussian pulse propagation in spatially dispersive

media analogous to that of Garrett and McCumber in the local case. There we considered frequency regimes far from resonance: cases 1 and 3,  $(\omega/\omega_0) \gg 1$  and  $\ll 1$ , respectively; and also in the pseudo-gap region  $\omega_0 < \omega < \omega_l$ . The pulse is characterized by  $\Gamma\tau \gg 1$ . Equations (8), (10), (14), and (17) show that in the various frequency regimes mentioned above, the Gaussian pulse propagates substantially as a Gaussian both on upper and lower polariton branches. In general, there will be a shift in the peak of the packet, and a change in full width at half maximum, as given in those equations.

Close to exciton resonance but above the longitudinal mode frequency ( $\omega_l$ ), our numerical study (for CdS parameters) reveals the following (as given in

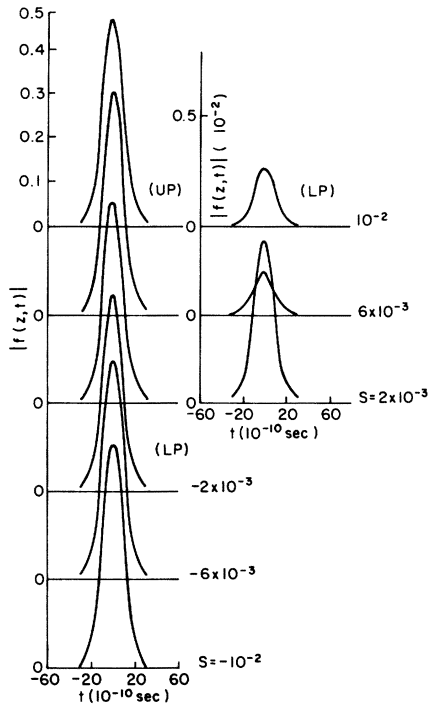


FIG. 8.  $|f(z,t)|$  for  $\Gamma\tau \gg 1$  case is plotted against  $t$  for various  $\bar{\omega}$ , ranging from  $S = (\bar{\omega} - \omega_0)/\omega_0 = -10^{-2}$  to  $10^{-2}$ . Here  $z = 10^{-4}$  cm. Parameters for CdS are defined in the text.

Sec. III): For  $\Gamma\tau \gg 1$  we obtain a symmetric power spectrum as shown in Fig. 1. As  $z$  is changed, the shape of the power spectrum remains unchanged. A slight asymmetry in the power spectrum is observed for the case  $\Gamma\tau = 1$  as shown in Fig. 2. For the case

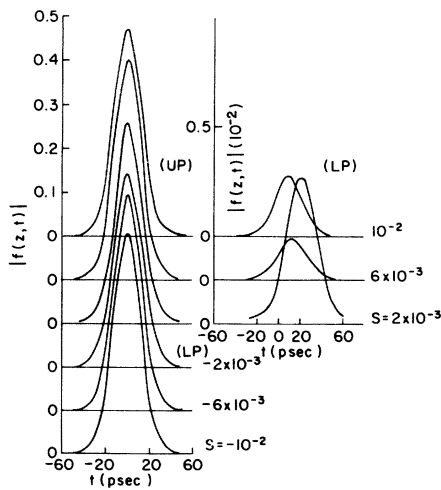


FIG. 9. Same as Fig. 8 for the  $\Gamma\tau = 1$  case.

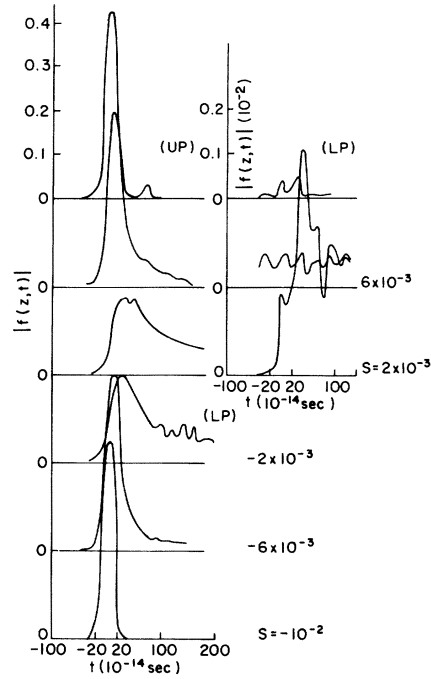


FIG. 10. Same as Fig. 8 for  $\Gamma\tau \ll 1$  case.

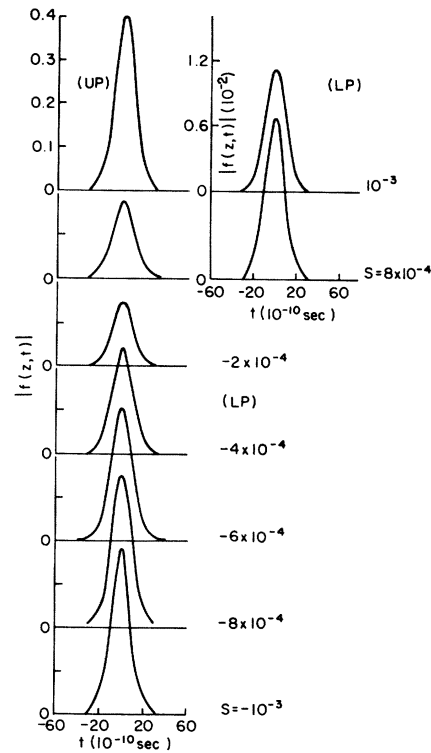


FIG. 11. Same as Fig. 8 for  $S = -10^{-3}$  to  $10^{-3}$ , i.e.,  $\bar{\omega}$  being very close to exciton resonance.

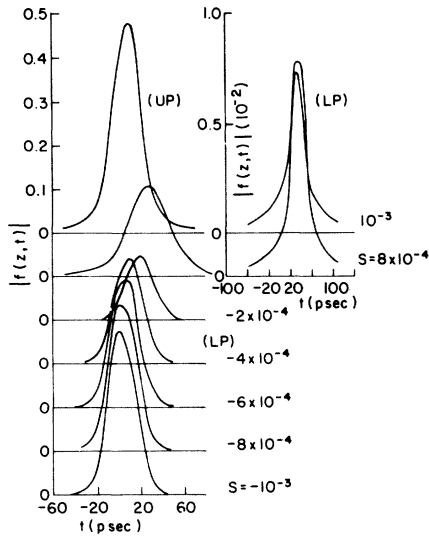


FIG. 12. Same as Fig. 9 for the  $\Gamma\tau=1$  case.

$\Gamma\tau \ll 1$  as shown in Fig. 3, as  $z$  is increased more and more asymmetry in the power spectrum can be noted. In this case an interesting “sharp cross over” is observed at  $\omega_l$  in the power spectrum from lower to upper polariton. This is shown in Fig. 4.

For  $\Gamma\tau \gg 1$ , the amplitude plots  $|f_1(z,t)|$  and  $f_2(z,t)|$  designated as UP and LP, respectively, show very little variation in the shape of the packet as crystal thickness  $z$  is changed from  $z = 10^{-6}$  to

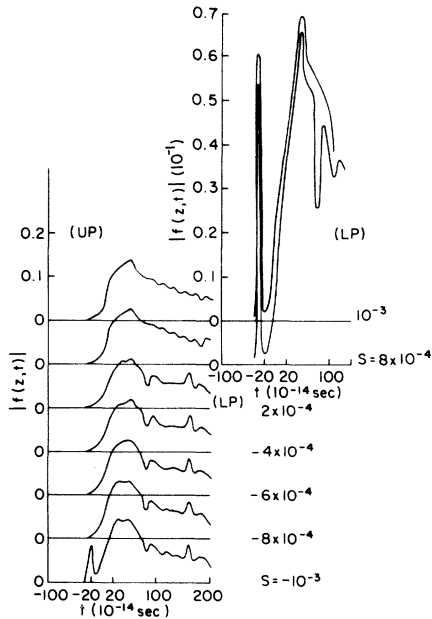


FIG. 13. Same as Fig. 9 for the  $\Gamma\tau \ll 1$  case.

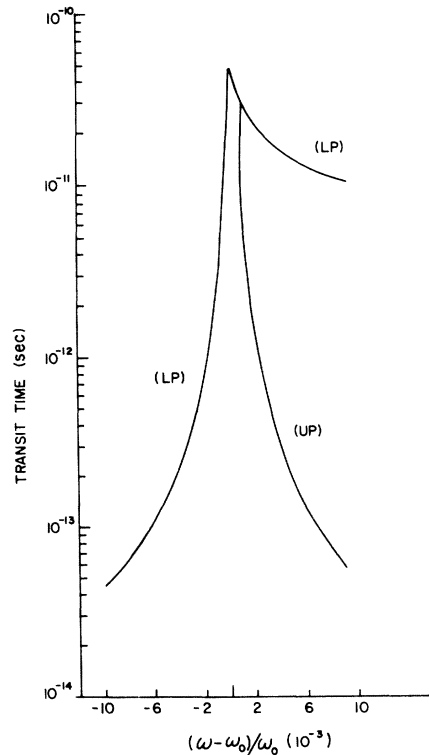


FIG. 14. Transit time of the Gaussian pulse through a  $1 \mu\text{m}$  thick medium with CdS parameters. Time in sec is plotted vs reduced frequency  $(\bar{\omega} - \omega_0)/\omega_0$ . This graph applies for cases  $\Gamma\tau \approx 1$  and  $\Gamma\tau \gg 1$ . Curve passes through calculated points, and coincides with the group velocity on each branch calculated from  $v_{g_j} = (d\omega_j/dk_r)$ .

$10^{-4}$  cm (see Fig. 5). This case corresponds to many oscillations in time as the packet is wide in time domain.

For  $\Gamma\tau = 1$ , the amplitude plots of  $|f_1(z,t)|$  and  $|f_2(z,t)|$  show relatively more variation in the shape of the packet as we increase the crystal thickness  $z$ , compared to the case  $\Gamma\tau \gg 1$ . It is useful to compare Figs. 5 and 6.

In the limit  $\Gamma\tau \ll 1$ , the packet gets more distorted as it propagates in the crystal as shown in Fig. 7. Notice here  $|f_1(z,t)|$  or UP becomes broadened and distorted as it moves in the crystal, i.e., as  $z$  is increased. Also,  $|f_2(z,t)|$  or LP, even for  $z = 10^{-6}$  cm does not appear Gaussian; it is rather flat and as it moves in the crystal more oscillations develop.

In the limit  $\Gamma\tau \gg 1$ , the pulse shape remains Gaussian as the frequency is varied through resonance; this is shown in Figs. 8 and 11. The pulse width remains substantially constant on both upper and lower polariton branches. Similar behavior is noted for  $\Gamma\tau = 1$ , as shown in Figs. 9 and 12. In this



case very little variation in pulse width is noted as we sweep across resonance (for example, a 26-psec pulse shows maximum variation of 4 psec). The  $\Gamma\tau \ll 1$  limit corresponds to considerable pulse distortion as demonstrated in Figs. 10 and 13. There is a great deal of structure in the lower polariton branch above resonance as seen in these figures.

Our analysis demonstrates that the velocity of the peak of the pulse is the group velocity in those cases where the pulse maintains an essentially Gaussian shape:  $\Gamma\tau \gg 1$  and  $\Gamma\tau = 1$ . This is shown in Fig. 14 for frequencies in the resonance region. We computed the transit time of the peak of the pulse wave packet as  $\bar{\omega}$  is varied through the resonance, which immediately gives the velocity of the peak. We plot in Fig. 14 the transit time  $t$  (sec) versus reduced frequency  $(\omega - \omega_0)/\omega_0$  for the cases  $\Gamma\tau \approx 1$  and  $\Gamma\tau \gg 1$  for UP and LP branches near exciton resonance for crystal thickness of  $1 \mu\text{m}$ . These delay times correspond to peak of the pulse propagating with group velocity. In these cases, the pulse shape remains substantially Gaussian, with very little variation in pulse width.

We shall compare our results now with more recent experiments, taking into account that our theory assumes a Gaussian initial pulse, whereas the pulse shapes achievable experimentally may not be of Gaussian shape.<sup>6</sup> Taking the experiments to cor-

respond to the cases  $\Gamma\tau \approx 1$ , our numerical results agree with the work of Refs. 7–10 which reported peak propagation at the group velocity  $v_{g_j} \equiv (d\omega_j/dk_r)$  in each branch. Also noteworthy is our calculated crossover from lower to upper polariton branch in the power spectrum as the laser is varied through the resonance frequency from below: This agrees with the experiments of Masumoto *et al.*<sup>8</sup> Finally, our theory predicts that the Gaussian shape will be preserved in cases  $\Gamma\tau \approx 1$  and  $\Gamma\tau \gg 1$  in spatially dispersive media. Taking into account the experimental uncertainties, this is in agreement with experiment.

It would clearly be desirable to obtain analytical expressions for pulse propagation in the spatially dispersive medium in different frequency ranges, including frequency-dependent coupling of the different branches. Work is continuing on these lines.

#### ACKNOWLEDGMENTS

We are happy to acknowledge useful discussions with Professor R. R. Alfano. This work was supported by Army Research Office Grant No. DAAG29-79-G-0040 and National Science Foundation Grant No. DMR78-12399, and a PSC-BHE City University of New York Faculty Research Award.

\*Present address: Department of Physics, Indiana University, Bloomington, IN 47405.

<sup>1</sup>M. Born and E. Wolf, *Principles of Optics* (Pergamon, Oxford, 1965).

<sup>2</sup>L. Brillouin, *Wave Propagation and Group Velocity* (Academic, New York, 1960).

<sup>3</sup>R. Loudon, *J. Phys. A* **3**, 233 (1970).

<sup>4</sup>C. G. B. Garrett and D. E. McCumber, *Phys. Rev. A* **1**, 305 (1970).

<sup>5</sup>M. D. Crisp, *Phys. Rev. A* **4**, 2104 (1971); **1**, 1604 (1970); *Phys. Rev. Lett.* **22**, 820 (1969).

<sup>6</sup>S. Chu and S. Wong, *Phys. Rev. Lett.* **48**, 738 (1982). See also A. Katz and R. R. Alfano, *Phys. Rev. Lett.* **49**, 1292 (1982) and S. Chu and S. Wong, *ibid.* **49**, 1293 (1982) in which some limitations of the experiments are discussed.

<sup>7</sup>R. G. Ulbrich and G. W. Fehrenbach, *Phys. Rev. Lett.* **43**, 963 (1979).

<sup>8</sup>Y. Masumoto, Y. Unuma, Y. Tanaka, and S. Shinoya, *J. Phys. Soc. Jpn.* **47**, 1844 (1979).

<sup>9</sup>T. Itoh, P. Lavallard, J. Reydellet, and C. Benoit a la

Guillaume, *Solid State Commun.* **37**, 925 (1981).

<sup>10</sup>Y. Segawa, Y. Aoyagi, K. Azuma, and S. Namba, *Solid State Commun.* **28**, 853 (1978); Y. Sewaga, Y. Aoyagi, T. Baba, and S. Namba, *J. Phys. Soc. Jpn. Suppl. A* **49**, 389 (1980).

<sup>11</sup>J. L. Birman and J. J. Sein, *Phys. Rev. B* **6**, 2842 (1972); J. J. Sein, Ph.D. thesis, New York University, 1969 (unpublished). For a recent discussion and review, see J. L. Birman, in *Excitons*, edited by E. I. Rashba and M. D. Sturge (North-Holland, New York and Amsterdam, 1982).

<sup>12</sup>G. S. Agrawal, D. N. Pattanyak, and E. Wolf, *Phys. Rev. Lett.* **27**, 1022 (1971); *Phys. Rev. B* **10**, 1477 (1974).

<sup>13</sup>A. A. Maradudin and D. L. Mills, *Phys. Rev. B* **7**, 2787 (1973).

<sup>14</sup>A. Puri and J. L. Birman, *Phys. Rev. Lett.* **47**, 173 (1981).

<sup>15</sup>M. J. Frankel and J. L. Birman, *Phys. Rev. A* **15**, 2000 (1977).